Chemical Engineering Journal 160 (2010) 63–71

Contents lists available at ScienceDirect

Chemical Engineering Journal

journal homepage: www.elsevier.com/locate/cej

Kinetics and equilibrium modeling of Se(IV) removal from aqueous solutions using metal oxides

R.R. Sheha*, E.A. El-Shazly

Nuclear Chemistry Department, Hot Lab. Center, Atomic Energy Authority, 13759 Cairo, Egypt

ARTICLE INFO

Article history:
Received 22 January 2010
Received in revised form 26 February 2010
Accepted 1 March 2010

Keywords:
Selenite removal
SiO_2
Fe_2O_3
Equilibrium modeling
Adsorption kinetics

ABSTRACT

The efforts in this study were devoted to investigate the removal efficiency of selenium from waste solutions using iron and silicon oxides. Experiments were carried out as a function of pH, equilibrium time, initial concentration and temperature. The adsorption process was very fast initially and the removal efficiency reached more than 90% after 3 h of contact for initial selenium concentration of 20 $\mu g\,L^{-1}$. High removal efficiency of selenite occurred in a wide range of pH (i.e., 2–8), but the efficiency decreased at pH values higher than 8. The immobilization of Se(IV) anions onto the surface of oxides may proceed through ligand-exchange interactions and/or inner-sphere complexation. Selenite interaction with oxide particles followed second-order kinetics with a correlation coefficient extremely high and closer to unity and the rate constant (k_s) had the values 7.69×10^{-5} and 3.59×10^{-5} g μg^{-1} min^{-1} for adsorption onto Fe_2O_3 and SiO_2, respectively. The values of equilibrium sorption capacity (q_e) are consistent with the modeled data and attained the value 1.8 mg g^{-1}. Kinetically, both pore and film diffusions are participating in ruling the diffusion of Se(IV) anions. Equilibrium adsorption data were analyzed using Freundlich, Langmuir and Dubinin–Radushkevich (D–R) isotherm models. Of the models tested, D–R isotherm expressions were found to give better fit to the experimental data compared to the other models. The revealed evidences argue that metal oxides could be used as efficient adsorbents for removal of selenium from wastewaters.

1. Introduction

Selenium (Se) is a natural trace element in environment has chemical and physical properties intermediate between those of metals and non-metals. It is an essential nutrient has very narrow margin between nutritionally optimal and potentially toxic dietary exposures for vertebrate animals [1]. It can increase activity of the free hydroxyl radicals (OH^-) that cause high oxidation stress harmful to living beings [2]. Accumulation of selenium in soils, aquifer sediments and drinking water can threaten the health of plants, wildlife, and humans [3]. The essential or toxic character of Se in living beings depends not only on its concentration in the circumstances, but also on the chemical form, which directly affects absorption and bioavailability [4,5].

Selenium is found in the effluents from thermal power stations, oil refineries, combustion from fossil fuels, roasting and refining of sulfide ores. Besides, it is widely used in various industries including production of glass, pigments, solar batteries, semiconductors and as catalyst in the synthesis of urea and urethane [6]. Selenium usually presents in amounts ranged from 0.1 to 20 ppm in aqueous effluents. Such levels are too high to permit safe environmental discharge and so the need to treating such effluents before discharge. The current drinking water regulation requires selenium levels to be less than 0.01 ppm. Selenium also presents in radioactive wastes by several radionuclides (^{75}Se, ^{79}Se, etc.). The release of the long-lived radionuclide ^{79}Se (half-life, 6.5×10^4 years) from waste depositories to the biosphere would have significant effects on the cumulative dose of radioactivity [7,8].

Environmentally, selenium can exist in different oxidation states as elemental selenium (Se^0), selenite (SeO_3^{2-}), selenide (Se^{2-}), selenate (SeO_4^{2-}) and organic selenium [9]. Selenite and selenate are the predominant chemical forms of selenium and thermodynamically stable [10]. Selenite (SeO_3^{2-}) is present in mildly oxidizing, neutral pH environments and typical humid regions. It is expected to be the predominant form at pH levels (~13.5) and redox potentials (~80 mV) [11]. Selenate is the predominant selenium form under ordinary alkaline and oxidized conditions [12].

The fully oxidized (+6) form has a tetrahedral oxyanion structure and exists in solution as selenate (SeO_4^{2-}) or biselenate ($HSeO_4^-$) that has pK_a of 1.7. The fully protonated selenic acid is a strong acid and does not occur in water [13]. The lower oxidized form of selenium, selenite, exists as pyramidal oxyanion selenite (SeO_3^{2-}). It is a weak diprotic acid can exist as H_2SeO_3, $HSeO_3^-$, or SeO_3^{2-} depending upon solution pH ($pK_{a1} = 2.64$ and $pK_{a2} = 8.4$) [14].

* Corresponding author. Tel.: +20 10 529 15 48.
E-mail address: rsheha68@yahoo.com (R.R. Sheha).

1385-8947/$ – see front matter © 2010 Elsevier B.V. All rights reserved.
doi:10.1016/j.cej.2010.03.004

A variety of treatment technologies have been reported for selenium removal from contaminated waters [15–17]. Adsorption onto metal oxides has been demonstrated as a promising method for selenium removal [18,19]. It was reported that adsorption of anions at oxide/water interfaces is commonly interpreted by surface complexation mechanism in which the anionic solutes were bonded to the surface reacting site to form either inner-sphere or ion-pair complex [20]. As a result, Fe_2O_3 and SiO_2 were chosen as substrates for Se removal in this study. These two oxides are ubiquitous in geological environments. SiO_2 is the most abundant oxide in earth crust and significantly applied in many industrial processes as water treatment plants [21]. The surface of SiO_2 is very acidic and has point of zero charges (pH_{PZC}) between 2 and 3, thus its ionized surface sites are positive at very low pH. On other hand, iron oxides that practically present in many natural media are good adsorbents for Se(IV) and Se(VI). They have high point of zero charge (8–10) making them positively charged over most pH ranges [19,22].

The sorption of metal ions on oxide surfaces is a major factor in controlling their mobility and bioaccessibility in aquatic systems. For such heterogeneous interactions, thermodynamic data only provide information about the final state of system, such as adsorption capacity and equilibrium constant, but kinetics deal with changes in chemical properties with time and concern especially with the rates of change. Therefore, to optimize the design of any adsorptive reactor for heterogeneous removal of metal ions, it is important to describe the nature of adsorption processes in such heterogeneous systems over a wide range of experimental conditions and time scales using various kinetic and isotherm models.

The objective of this study was to apply iron and silicon oxides adsorbents in selenite removal from aqueous solutions. Series of batch adsorption experiments were conducted to determine the effect of pH, adsorption time, temperature, and initial concentration on removal efficiency. Our goal was to investigate the adsorption behavior of Se(IV) under different conditions and to quantify the system kinetics using robust models.

2. Experimental

2.1. Materials

All chemical solutions were prepared using de-ionized water and analytical grade chemicals. Selenium, in form of SeO_2, was purchased from Aldrich. Selenite reference standard solution was attained from Thermo Fisher Scientific, UK. Iron and silicon oxides were obtained from NMA, Egypt. These oxides were washed with distilled water until a constant electrical conductivity was obtained. Then, they were immersed in methanol for 3 h, separated and dried at 50 °C for 24 h. The obtained substrates were then kept in a desiccator for further usage. Other chemicals were purchased from Adwic, Egypt. A potentiometric method was used to determine the point of zero charge (pH_{PZC}) for both adsorbents and values are listed in Table 1.

2.2. Selenium analysis

In all experiments, the concentration of selenium was determined by Atomic Absorption Spectrometer (AAS). Analysis was performed using Solaar-II M5 Atomic Absorption Spectrometer from Thermo Fisher Scientific Inc., Cambridge, UK. The instrument was equipped with a Vapor Generation Accessory of type Vapor Kit VP-100. Using this Kit, Se(IV) was reduced by $NaBH_4$ to generate H_2Se, which was stripped by N_2 carrier gas (flow rate = 200 mL min^{-1}) and introduced into an acetylene-flame-heated quartz cell (fuel flow rate 1.0 L min^{-1}) to achieve an absorbance reading at a wavelength of 196.0 nm. Two different treatments were performed to differentiate Se(IV) and the total Se(IV + VI). Se(IV) was quantified by acidifying an aliquot of the sample with 0.5 M HCl and analyzing it directly by HSAAS. Under the same conditions, we verified that Se(VI) could not be reduced by $NaBH_4$ and thus could not be detected. To determine Se(IV + VI), aliquots of sample were acidified with 0.5 M HCl, and reduction of Se(VI) to Se(IV) was achieved by heating the acidified solutions at 70 ± 2 °C for 50 min. Total Se was then determined by HSAAS, and Se(VI) was given by the difference between the amounts of Se(IV + VI) and of Se(IV). Analysis with and without prereduction allowed us to verify that no oxidation occurred when selenite ions were employed in adsorption experiments [23].

Table 1
Physico-chemical properties of the applied metal oxides.

Material	Surface area ($m^2\ g^{-1}$)	pH_{PZC}
Iron oxide	98.2	6.4
Silicon oxide	198.5	3.1

2.3. Adsorption studies

1 mg L^{-1} selenium (IV) stock solution was prepared by dissolving analytical grade SeO_2 into 250 mL de-ionized water containing ~0.5 mL concentrated hydrochloride acid. A working solution of 20 ppm was prepared using the stock solution for the adsorption experiments. Suspensions containing 1.0 g of oxide particles and 100 mL solution traced with a prefixed initial concentration of Se(IV) in sealed glass flasks, were aged at room temperature (29 ± 1 °C) using a thermostated water bath shaker of Stuart Scientific SBS-30 type, UK. Aliquots were taken, at appropriate time intervals as necessary, centrifuged and the concentration of Se(IV) was determined using HSAAS. Additional batch of experiments was conducted as a function of pH value over the range 2–11. If necessary, the pH value was initially adjusted using 0.1 M HCl and/or 0.1 M NaOH solutions. The suspensions were aged for equilibrium and then centrifuged. The supernatants were separated and final pH value and Se concentration were determined. The pH values were measured using MA-235 digital pH meter from Mettler Toledo, UK.

Adsorption isotherm experiments were also performed using solutions spiked with different initial concentrations of Se(IV) ranged from 10 up to 50 ppm. These solutions were dosaged with 10 g L^{-1} oxide substrates and their initial pH values were ~4.0 ± 0.5. The mixtures were stirred for equilibrium, centrifuged and the supernatants were separated and subjected for metal concentration measurements. The uptake percent of Se(IV) adsorbed onto oxide particles was calculated using the relation:

$$Se(IV)_{adsorbed}\,\% = \frac{[Se(IV)]_{in}[Se(IV)]_{eq}}{[Se(IV)]_{in}} \times 100 \quad (1)$$

where $[Se(IV)]_{in}$ and $[Se(IV)]_{eq}$ are the initial and equilibrium concentrations of Se(IV) in the solution (μg L^{-1}). All experiments were performed at room temperature of 29 ± 1 °C and pH of ~4.0 ± 0.5 in duplicate and the averaged values were taken.

3. Results and discussion

3.1. Adsorption study

3.1.1. Effect of pH

The uptake of Se(IV) as a function of hydrogen ion concentration was examined over a pH range of 2–11.5 and the revealed data are shown in Fig. 1. The removal efficiency of Se(IV) onto metal oxides was not significantly affected by pH increase in the range of 2–8 approaching a plateau at this range. Increasing pH values higher than 8 dropped the removal percent to <5% at pH of 11.5.

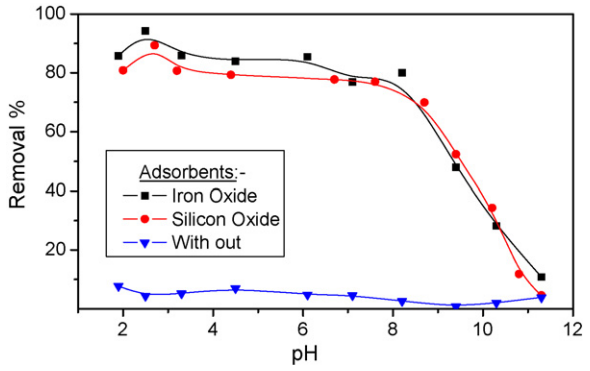

Fig. 1. Adsorption of Se(IV) anions onto metal oxides as a function of pH (time = 6 h, temperature = 29 ± 1 °C and adsorbent wt. = 10 g L^{-1}).

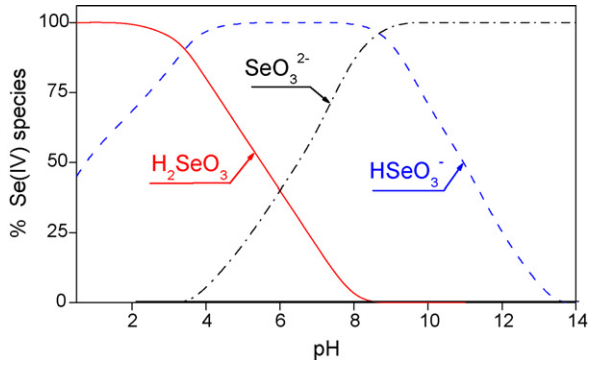

Fig. 3. Speciation diagram of selenite in aqueous solutions.

The relationship between initial and equilibrium pH values for selenite adsorption is illustrated in Fig. 2. The plots clarify that the studied metal oxides have a pH buffering capacities over the pH range ~4–9. If no specific adsorption from aqueous solution occurred, acidic as well as basic aqueous solutions were buffered after reaction with metal oxides to pH values 5.5–6. These buffering characteristics of metal oxides are a result of acid–base reactions of the reactive surface sites on oxide surface [24]. Depending upon solution pH, the oxide surface can act as a weak acid or base and gain or lose proton (i.e. it can undergo protonation or deprotonation). Therefore, the following reactions are expected to occur at the surface of oxides:

$$\equiv SO^- + H^+ \rightleftharpoons \equiv SOH \quad (2)$$

$$\equiv SOH + H^+ \rightleftharpoons \equiv SOH_2^+ \quad (3)$$

where ≡SOH represents a singly protonated oxide site. The above reactions reveal that increasing the concentration of protonated surface oxide sites result in increase the adsorption extent of selenium anions that proposed to occur according to the following equilibria:

$$\equiv SOH_2^+ + SeO_3^{2-} + H^+ \rightleftharpoons \equiv S\text{–}O\text{–}Se(O)\text{–}OH + H_2O \quad (4)$$

Thus, when the initial pH was low, the equilibrium pH increased due to the acid–base interactions of these oxides and this suggests the contribution of surface complexes formation, to some extent, in the overall adsorption mechanism. The high initial pH values were also buffered by adsorption of OH^- directly from the solution onto oxide surface and so the final pH values decreased.

Fig. 3 presents the relationship between the relative amounts of selenium ionic species and solution pH calculated by visual MINTEQ software [25]. The figure clarifies that Se(IV) species present in aqueous solution are mainly in the form H_2SeO_3 (seleniuos acid) ions up to pH 3.5. The negatively charged biselenite ($HSeO_3^-$) appears in pH range 3.5 ~ 9, while the selenite species (SeO_3^{2-}) predominates at pH values higher than 9 [26].

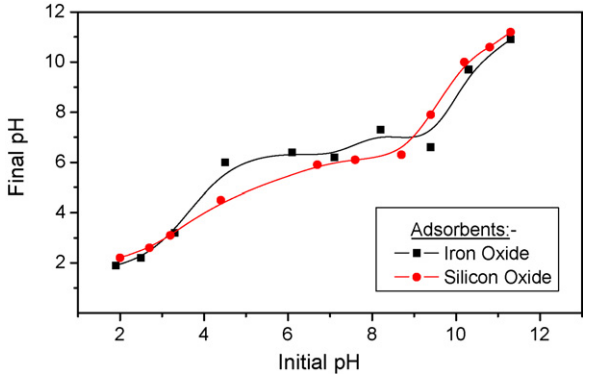

Fig. 2. A plot of initial and final pH values for adsorption of Se(IV) anions onto metal oxides (time = 6 h, temperature = 29 ± 1 °C and adsorbent wt. = 10 g L^{-1}).

It was reported that the adsorption of Se(IV) on metal oxides is independent of the background electrolyte strength wherever the adsorption of selenate is dependent on it [22,23]. The background electrolyte concentration influences the double layer thickness and interface potential, thereby affecting the binding of the adsorbing species. Outer-sphere complexes are expected to be more susceptible to ionic-strength variations than inner-sphere complexes, since the background electrolyte ions are placed in the same plane as the outer-sphere complexes. Consequently, adsorption of SeO_3^{2-} might imply the formation of inner-sphere complexes [20].

These evidences argue that electrostatic attraction between Se(IV) anions and the positive protonated surface sites of metal oxides (≡S–OH_2^+) is the favorable interaction over low initial pH range. Also, surface complexation is a common accepted mechanism for adsorption of Se anions by oxide surfaces, involving adsorption of the species SeO_3^{2-} (selenite) and $HSeO_3^-$ (biselenite) on the surface by ligand-exchange that can be represented as follow [6]:

$$\equiv S\text{–}OH + H^+ + SeO_3^{2-} \rightleftharpoons \equiv S\text{–}SeO_3^- + H_2O \quad (5)$$

$$\equiv S\text{–}OH + 2H^+ + SeO_3^{2-} \rightleftharpoons \equiv S\text{–}HSeO_3 + H_2O \quad (6)$$

where ≡S–OH is a surface hydroxyl group, ≡S–SeO_3^- and ≡S–$HSeO_3$ are the adsorbed selenite species. The above reactions suggest that the removal of anions from solution by adsorption on metal oxide surfaces is strongly influenced by pH of the system.

The high Se(IV) adsorption occurred at low pH values (≥3.5) suggests the removal of selenium species from aqueous solution through electrostatic and/or surface complexation interactions. Both mechanisms work together to a significant extent and play a critical role in the overall removal of Se(IV) although it was difficult to quantitatively estimate the extent of removal referred to any of them. At this range (pH values ≥3.5), the initial pH value is lower than the point of zero charge for both oxides (pH_{PZC} equals 3.1 for SiO_2 and 6.4 for Fe_2O_3), and so the surface sites are highly protonated (≡SOH_2^+) and participate in electrostatic interactions with the negative biselenite ($HSeO_3^-$) anions. The neutral seleniuos acid (H_2SeO_3) was removed through ligand-exchange mechanism. The lack of inner-sphere complex formation at pH ≥ 3.5 was caused by changes in the corundum surface of the oxides at low pH or secondary Se(IV) precipitate formation [13].

With further increase in pH up to 8, the surface of SiO_2 becomes negatively charged and hence the electrostatic contribution is not evident for Se(IV) adsorption. This evidence shows that inner-sphere complexation (covalent binding of selenite anions with the surface sits) is the relevant mechanism taking place in adsorption

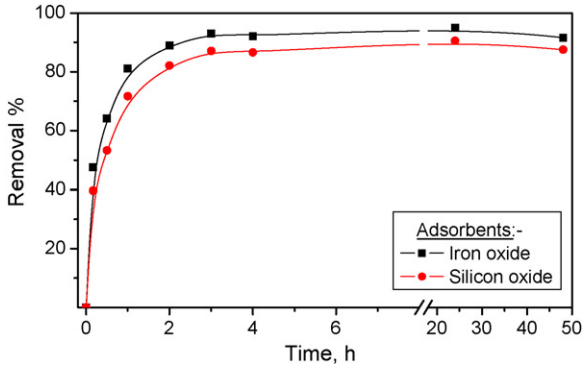

Fig. 4. Adsorption of Se(IV) anions onto metal oxides at different time intervals (pH ~ 4, temperature = 29 ± 1 °C and adsorbent wt. = 10 g L^{-1}).

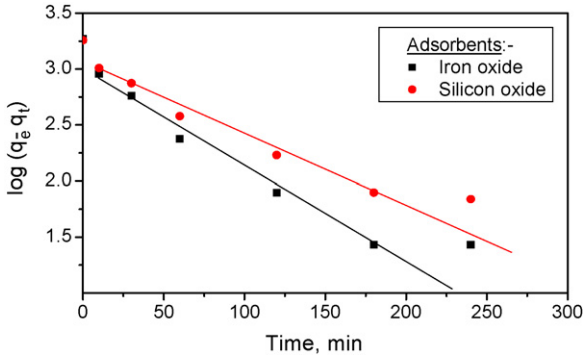

Fig. 5. Lagergren plots for adsorption of Se(IV) anions onto metal oxides (pH ~ 4, temperature = 29 ± 1 °C and adsorbent wt. = 10 g L^{-1}).

of $HSeO_3^-$ and SeO_3^{2-} anions over pH range 3.5–8.0. On other hand, the point of zero charge for Fe_2O_3 oxide (pH_{PZC} equals 6.4), is still higher than the working pH value, and so their surface sites are positively protonated and participate in electrostatic interactions with the negative biselenite ($HSeO_3^-$) and selenite (SeO_3^{2-}) anions. Hence, the removal of Se(IV) from aqueous solutions, at these conditions, was suggested to be achieved through electrostatic and inner-sphere complexation interactions. Several inner-sphere complexes could be formed at the surface of ferric oxides: monodentate (≡S–O–Se(O)OH, ≡S–O–Se(O)O^- or ≡S–O–Se(O^-)$_2$OH), bidentate (≡S–O)$_2$–SeO and tridentate (≡S–O)$_3$–SeOH. Earlier studies have shown that selenite anions form inner-sphere complexes onto ferric oxy-hydroxides using IR and EXAFS spectroscopy [7,22,27]. Due to the buffering capacity of both oxides over this pH range, their removal efficiency was not significantly affected by pH increase. A similar trend was observed by other investigators [18].

At high pH values (8–11.5), a steady decrease in the percentage of adsorption was observed. At this pH range, the surface sites of the used oxides are deprotonated attaining a negative charge (≡S–O^-) and the high negatively charged selenite (SeO_3^{2-}) species prevail in this range. Therefore, the repulsion between SeO_3^{2-} species and ≡S–O^- sites in addition to the intermolecular competitiveness between OH^- and selenite anions for the adsorption sites highly depressed the removal efficiency. This behavior is coincident with that reported for adsorption of selenite onto other adsorbents [6,12,28].

3.1.2. Effect of contact time

The effect of time on the removal efficiency of Se(IV) is shown in Fig. 4. It can be seen that the rate of Se(IV) uptake was initially quite high, followed by a much slower subsequent removal rate leading gradually to an equilibrium condition. About 80% of the Se(IV) was removed during the first 2 h of the reaction, while only a very small part of the additional removal occurred during the rest of contact. These results reflect the efficiency of the used metal oxides for removal of Se(IV) from aqueous solution in a wide range of concentrations.

The rapid adsorption of Se(IV) by the applied metal oxides was perhaps attributed to the surface site initially available for Se(IV) adsorption is very large compared to the concentration of Se(IV) ions and consequently, the rate of adsorption was very high. However, with increasing coverage, the fraction of adsorption sites in oxide surface rapidly diminished and Se(IV) ions had to compete among themselves for the adsorption sites. This results in a slowing down of the interaction progress and the rate of adsorption becomes predominantly dependent on the rate at which Se(IV) ions transport from the bulk to the sorbent–adsorbate interface. The kinetics of the interaction were thus likely to be dependent on different rate processes as the interaction time increases. Generally, efficiency amounted to 94 and 89% for Se(IV) removal using iron and silicon oxides was attained after ~3 h of contact.

3.2. Adsorption kinetic modeling

The kinetics of adsorption process were studied by carrying out a set of adsorption experiments between Se(IV) and oxide adsorbents at constant temperature and monitoring the amount adsorbed with time. The adsorption kinetics normally include two phases: a rapid removal stage followed by a much slower stage before the equilibrium is established. Assuming pseudo-first-order kinetics, the rate of the adsorptive interactions can be evaluated using the simple Lagergren model equation [29]:

$$\log(q_e - q_t) = \log\ q_e - \frac{k_f t}{2.303} \quad (7)$$

where q_e and q_t are the amount of Se(IV) adsorbed per unit mass (mg g^{-1}) at equilibrium and at any time t and k_f is the pseudo-first-order adsorption-rate constant (min^{-1}). The values of k_f could be obtained by plotting log ($q_e - q_t$) versus t for adsorption of Se(IV) at 29 °C and pH ~ 4.0 and the data are represented in Fig. 5. The plots show straight lines have a good linearity. The values of first-order rate constant (k_f) and correlation coefficient (R^2) obtained

Table 2
Kinetic parameters for adsorption of Se(IV) anions onto metal oxides.

Kinetic parameters		Adsorbent	
Model	Parameters	Iron oxide	Silicon oxide
Pseudo first order (Lagergren)	k_f (min^{-1})	0.022	0.016
	R^2	0.987	0.984
	SD	±0.123	±0.099
Pseudo-second order	k_s (g μg^{-1} min^{-1})	7.69×10^{-5}	3.59×10^{-5}
	h (μg g^{-1} min^{-1})	266.6	130.2
	R^2	0.999	0.999
	SD	±0.003	±0.008

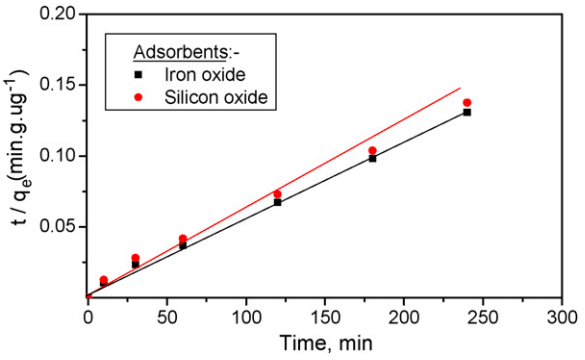

Fig. 6. Pseudo-second-order plots for adsorption of Se(IV) anions onto metal oxides (pH ~ 4, temperature = 29 ± 1 °C and adsorbent wt. = 10 g L^{-1}).

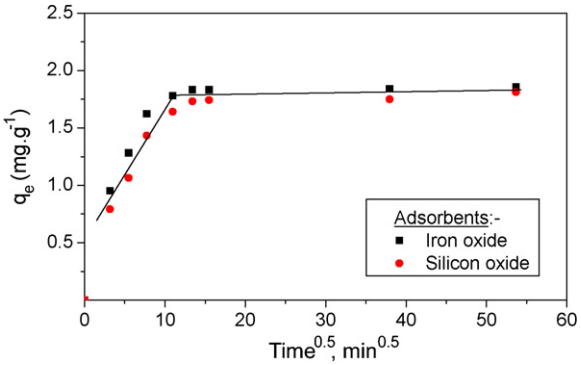

Fig. 7. Weber–Morris plots for adsorption of Se(IV) anions onto metal oxides (pH ~ 4, temperature = 29 ± 1 °C and adsorbent wt. = 10 g L^{-1}).

from these plots are listed in Table 2. The oxide adsorbents differ very little in the rates of uptake of Se(IV) ions. The differences in the kinetics between the two oxides could thus be attributed to the structural differences existing between them. The first order mechanism suffered from inadequacies when applied to Se(IV) adsorption on the metal oxides. One of the major discrepancies was observed when q_e values obtained from Lagergren plots were compared with the experimental q_e values, Table 3. The experimental q_e values differed from the corresponding theoretical values for both iron and silicon oxides. Thus, good linearity of Lagergren plots is not guarantee that the interactions of Se(IV) with the applied oxides will follow first order kinetics.

In order to find a more reliable description of the kinetics, second-order kinetic equation was applied. The pseudo-second-order kinetics can be represented by the following linear equation [30].

$$\frac{t}{q_t} = \frac{1}{k_s {q_e}^2} + \frac{1}{q_e} t \tag{8}$$

where k_s is the second-order rate constant (g μg^{-1} min^{-1}). The kinetic plots of t/q_t versus t for Se(IV) removal are shown in Fig. 6. The relationship is linear and the correlation coefficient (R^2) suggests a strong relationship between the model parameters and explains that the adsorption process follows pseudo-second-order kinetics. The equilibrium adsorption capacity (q_e), the initial adsorption rate (h) that represented as $h = k_s {q_e}^2$, the pseudo-second-order constant (k_s) along with correlation coefficient were determined and listed in Table 2. From these data, it was observed that, the calculated correlation coefficient is extremely high and closer to unity for pseudo-second-order kinetic model than for pseudo-first-order kinetic model. The calculated equilibrium adsorption capacity (q_e) is consistent with the experimental data, Table 3. Therefore, the adsorption reaction could be approximated more favorably by the pseudo-second-order kinetic model. These results showed that the adsorption process followed the pseudo-second-order kinetic and suggested that chemisorption, through sharing or exchange of electron between adsorbent and adsorbate, is the rate-limiting mechanism in the overall adsorption of Se(IV) anions onto the surface of both oxides [31].

Table 3
Experimental and modeled values of equilibrium adsorption capacity (q_e) of the applied metal oxides towards Se(IV) anions.

Adsorbent	q_e (μg g^{-1})		
	Experimental	Lagergren	Second order
Iron oxide	1853	1241	1862
Silicon oxide	1796	1306	1810

The solute transport from a solution phase to the surface of oxide particles occurs in several steps such as external diffusion, surface diffusion, pore diffusion and adsorption on the pore surface, or a combination of more than one step. The overall adsorption process may be controlled either by one or more of these steps. In rapidly stirred batch adsorption, the diffusive mass transfer can be related by an apparent diffusion coefficient, which will fit the experimental adsorption-rate data. Generally, a sorption process is diffusion controlled if its rate is dependent upon the rate at which components diffuse towards one another. The possibility of intra-particle diffusion was explored by using the intra-particle diffusion model given by Weber–Morris and represented by the equation [32]:

$$q_t = k_{id} t^{0.5} + C \tag{9}$$

where k_{id} is the intra-particle diffusion rate constant (mg g^{-1} min$^{-0.5}$) and C is a constant (mg g^{-1}) gives an idea about the thickness of the boundary layer, i.e., larger the value of C the greater is the boundary layer effect. If Weber–Morris plot of q_t versus $t^{0.5}$ gives a straight line, then the adsorption process is controlled by intra-particle diffusion only. However, if the data exhibit multi-linear plots, then two or more steps influence the adsorption process. Weber and Morris plots of Se(IV) adsorbed per unit mass of adsorbent versus $t^{0.5}$ for both oxides are given in Fig. 7. The slope of these plots is defined as a rate parameter that characteristic to the rate of adsorption in region where intra-particle diffusion is the controlling rate. The graphs reveal data points related by two straight lines, the first portion depicting macropore diffusion and the second representing micropore diffusion. Extrapolation of the linear portions of the plots back to the y-axis gives the intercepts, which provide a measure of the boundary layer thickness. The deviation of single straight lines from the origin may be due to difference in rate of mass transfer in the initial and final stages of adsorption. Further, such deviation of straight line from the origin indicates that the pore diffusion is not the sole rate-controlling step. The adsorption data for q_e versus $t^{0.5}$ for the initial period show curvature, usually attributed to boundary layer diffusion effects or external mass transfer effects. The values of model parameters were calculated from the slops of the linear plots obtained and given in Table 4. The intra-particle diffusion rate constant (k_{id}) had the values 8.57×10^{-2} and 9.36×10^{-2} mg g^{-1} min$^{-0.5}$ for Se(IV) adsorption on Fe_2O_3 and SiO_2, respectively. The correlation coefficient (R^2) had values ranged from 0.948 to 0.971. It is likely supposed that a large number of Se(IV) ions diffuse into the pores before being adsorbed. Significantly, the plots did not have a zero intercept as proposed by Eq. (9) indicating that intra-particle diffusion might not be the controlling factor in determining the kinetics of the process.

Table 4
Intra-particle and liquid film diffusion models parameters for adsorption of Se(IV) anions onto metal oxides.

Kinetic parameters		Adsorbent	
Model	Parameters	Iron oxide	Silicon oxide
Intra-particle diffusion	k_{id} (mg g^{-1} min$^{-0.5}$)	8.57×10^{-2}	9.36×10^{-2}
	Intercept	0.796	0.570
	R^2	0.948	0.971
	SD	±0.135	±0.109
Liquid-particle diffusion	k_{fd} (min^{-1})	0.0206	0.0151
	Intercept	−0.269	−0.218
	R^2	0.995	0.994
	SD	±0.067	±0.054

When the transport of the solute molecules from liquid phase up to solid phase boundary plays the most significant role in adsorption, the liquid film diffusion model may be applied using the equation described bellow [33]:

$$\log(1-F) = -\frac{K_{fd}}{2.303}\, t \tag{10}$$

where F is the fractional attainment of equilibrium ($F = q_t/q_e$) and k_{fd} is the film diffusion rate constant. A linear plot of log $(1-F)$ versus t with zero intercept would suggest that the kinetics of the adsorption process is controlled by diffusion through the liquid film surrounding the solid sorbents. The plots of log $(1-F)$ versus t are illustrated in Fig. 8. The curves exhibit linear plots with a correlation coefficient values ($R^2 = 0.995$) and intercepts of −0.269 and −0.218 for Se(IV) adsorption on Fe_2O_3 and SiO_2, respectively. The rate constant for liquid film diffusion, k_{fd}, was in the range of 0.0151–0.0206 min^{-1}, Table 4. The non-zero intercepts again show that despite giving linear plots, the predictions of the model will have only limited applicability in adsorption of Se(IV) on the applied metal oxides. Finally, the kinetics of interaction of Se(IV) with the oxide surfaces do not appear to be straight forward, second-order mechanism is the more likely adsorption kinetics and both pore and film diffusions are participating in ruling the diffusion of solute ions.

3.3. Adsorption isotherm

There are many isotherms can be used for modeling the adsorption process in heterogeneous systems. Of these models, Freundlich, Langmuir and Dubinin–Radushkevich (D–R) isotherms are considered in this study and their parameters were obtained from the logarithmic form of isotherm equations. The equations for Freundlich, Langmuir and Dubinin–Radushkevich isotherms models are expressed respectively by [24]:

$$q_e = K_F C_e^{\,1/n} \tag{11}$$

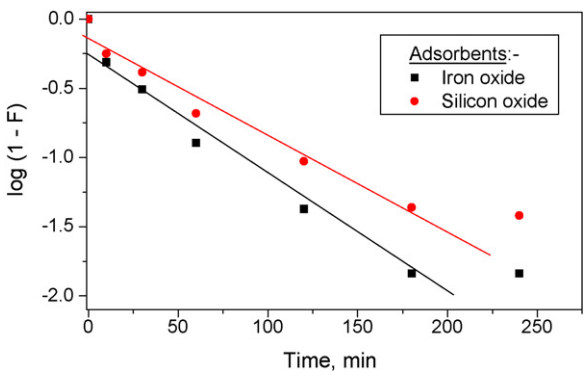

Fig. 8. Boyd plots for adsorption of Se(IV) anions onto metal oxides (pH ~ 4, temperature = 29 ± 1 °C and adsorbent wt. = 10 g L^{-1}).

$$q_e = \frac{Q_m K_L C_e}{1 + K_L C_e} \tag{12}$$

$$q_e = Q_m \exp(-K_D \varepsilon^2) \tag{13}$$

where q_e is the amount of selenite anions adsorbed per unit weight of oxide adsorbent at equilibrium (mg g^{-1}), C_e is the equilibrium concentration of Se(IV) in solution (μg L^{-1}), Q_m is the maximum sorption capacity of the oxide adsorbent (mg g^{-1}), K_F is Freundlich isotherm constant (mg$^{(1-1/n)}$ L$^{1/n}$ g^{-1}) that is indicative to the relative adsorption capacity, $1/n$ is Freundlich isotherm exponent constant related to the adsorption intensity, K_L (L mg^{-1}) is Langmuir isotherm constant related to the free energy of adsorption ($K_L \alpha\, e^{-\Delta G/RT}$). The constant K_D (mol^2 kJ^{-2}) gives the mean free energy E (kJ mol^{-1}) of adsorption per molecule of selenite when it is transferred to the surface of oxide from infinity in the solution, ε is Polanyi potential constant given as $RT\ln(1 + 1/C_e)$, where R is the universal gas constant equals to 8.3145 J mol^{-1} K^{-1}, T is the absolute temperature (K).

Freundlich model was chosen to estimate the adsorption intensity of selenite anions on the oxide surface. The experimental data were logarithmically plotted using the linear Freundlich isotherm equation (*data are given in* Appendix A). The obtained straight lines indicate that the adsorption of Se(IV) onto both metal oxides fit the investigated model. The numerical values of model parameters, evaluated at different temperatures from the slope and intercept of the linear plots, along with the correlation coefficient are given in Table 5. The Freundlich isotherm parameter $(1/n)$, that measures the adsorption intensity of Se(IV) ions on the applied oxides, showed values less than unity (0.69–0.99) indicating that the isotherms could be characterized by a convex Freundlich isotherm. This implies that a significant adsorption might take place even at high metal ion concentration. The K_F values of Se(IV) adsorption onto iron oxide are greater than that for adsorption onto silicon oxide. These date confirm that iron oxide has greater adsorption tendency towards the Se(IV) ions than silicon oxide.

Langmuir model parameters were determined from the slope of the linear relations obtained by plotting $1/q_e$ against $1/C_e$ and their values along with the correlation coefficient are given in Table 5. The adsorption capacity, Q_m, which is a measure of the capacity corresponding to complete monolayer coverage showed values for iron oxide higher than that for silicon oxide. The values of Langmuir constants (Q_m and K_L) decreased with rising temperature for both oxide adsorbents implying the depress in both capacity and intensity of adsorption at higher temperatures and clarifying the exothermic nature of the adsorption process. The estimated adsorption capacities (Q_m) are much higher than the value previously reported for Fe-GAC (2.58 mg g^{-1}) and for tropical soil (0.145 mg g^{-1}) as an adsorbent for selenite removal [1]

Furthermore, the favorability of adsorption of Se(IV) anions on these oxides was tested using the essential features of Langmuir isotherm model, expressed in terms of a dimensionless constant called "separation factor (S_F)" which is defined by the expression

Table 5
Isotherm model parameters for adsorption of Se(IV) anions onto metal oxides.

Isotherm Model		Adsorbent					
Model	Parameters	Iron oxide			Silicon oxide		
		303 K	313 K	323 K	303 K	313 K	323 K
Freundlich	K_F ($mg^{(1-1/n)}L^{1/n}g^{-1}$)	1.092	0.664	0.336	0.897	0.571	0.460
	$1/n$	0.99	0.93	0.85	0.74	0.70	0.69
	R^2	0.997	0.971	0.999	0.992	0.986	0.948
	SD	±0.023	±0.075	±0.012	±0.028	±0.039	±0.073
	Δq (%)	6.76	13.68	17.13	11.76	7.19	13.51
Langmuir	Q_m ($mg\,g^{-1}$)	8.47	7.30	6.52	7.06	6.38	4.58
	K_L ($L\,mg^{-1}$)	0.125	0.101	0.052	0.132	0.098	0.090
	S_F	0.997	0.998	0.998	0.997	0.998	0.999
	R^2	0.998	0.971	0.949	0.992	0.978	0.928
	SD	±0.024	±0.110	±0.022	±0.030	±0.054	±0.102
	Δq (%)	26.85	22.45	16.79	7.85	18.17	14.77
Dubinin–Radushkevich (D–R)	Q_m ($mmol\,g^{-1}$)	0.109	0.097	0.089	0.092	0.078	0.054
	K_D ($mol^2\,kJ^{-2}$)	9.42×10^{-9}	9.88×10^{-9}	1.25×10^{-8}	8.07×10^{-9}	9.78×10^{-9}	1.53×10^{-8}
	E_a ($kJ\,mol^{-1}$)	7.29	7.11	6.32	7.87	7.15	5.72
	R^2	0.997	0.961	0.992	0.984	0.969	0.979
	SD	±0.024	±0.086	±0.040	±0.041	±0.057	±0.054
	Δq (%)	10.12	3.41	5.88	6.86	1.64	4.25

[34]:

$$S_F = \frac{1}{1 + K_L C_o} \tag{14}$$

where K_L is Langmuir constant and C_o is the initial concentration of Se(IV) anions. The values of S_F parameter were determined and given in Table 5. These values are less than unity indicating that the adsorption is favorable and the used oxide adsorbents are optimum for removal of selenite ions from waste solutions.

Although Freundlich and Langmuir constants K_F and Q_m have different meanings, they led to the same conclusion about the correlation of the experimental data with the sorption model. The basic difference between K_F and Q_m is that Langmuir isotherm assumes sorption free energy independent of both surface coverage and formation of monolayer, whereas the solid surface reaches saturation while the Freundlich isotherm does not predict saturation of the solid surface by the sorbate, and therefore, the surface coverage being mathematically unlimited. In conclusion, Q_m is the monolayer sorption capacity while K_F is the relative sorption capacity or sorption power.

Dubinin–Radushkevich isotherm parameters values were obtained by graphical representation of the linearized form of model equations and data are given in Table 5 (*see* Appendix A). Closer inspection of these data shows that the maximum sorption capacity (Q_m) of the oxides applied for Se(IV) removal exhibit higher values for iron oxide that for silicon oxide and both decrease with temperature. The values of porosity factor (K_D) are less than unity implying the oxide surfaces to have fine micropores and indicate a surface heterogeneity that may be arisen from the pore structure as well as adsorbate–adsorbent interactions.

The apparent energy of adsorption (E, $kJ\,mol^{-1}$), defined as the free energy change when one mole of ion is transferred from infinity in the solution to the surface of oxide, is calculated using the equation [35]:

$$E = (-2K_D)^{-1/2} \tag{15}$$

The magnitudes of E were ranged from 5.7 to 7.9 $kJ\,mol^{-1}$ for Se(IV) adsorption onto both metal oxides, Table 5. Comparable values were reported for adsorption of selenite on calcined Mg/Fe LDH [6]. These values are less than 8 $kJ\,mol^{-1}$ and so clarify participation of physical forces in the overall adsorption mechanism [36].

In order to compare the validity of isotherm equations more definitely, a normalized standard deviation, Δq (%) is calculated as follows [37]:

$$\Delta q\ (\%) = 100 \times \sqrt{\frac{\sum [(q_e^{exp} + q_e^{cal})/q_e^{exp}]^2}{n-1}} \tag{16}$$

where the superscripts 'exp' and 'cal' show the experimental and calculated values and n is the number of measurements. The validity of the isotherm models was tested by comparing the experimental and calculated data at different temperatures and the values of Δq (%) are given in Table 5. Generally, the different isotherm models are appropriate in their merits in describing the potential of the oxide adsorbents for removal of Se(IV) ions from waste solutions. Based on the normalized standard deviation Δq values, Dubinin–Radushkevich isotherm model (D–R) mostly provide a better fit of experimental data while the other two models produce a satisfactorily fit over the entire range of concentration. This suggests that some heterogeneity in the surface of applied oxides will play a role in immobilization of selenite anions.

3.4. Adsorption thermodynamic

The adsorption isotherms of Se(IV) removal from waste solutions using metal oxides at different temperatures showed regular and positive plots concaved to the concentration axis. These plots illustrate initially rapid adsorption process, reflecting the efficiency of oxide adsorbents for the removal of selenite from aqueous solution. The effect of temperature on uptake of Se(IV) anions was evaluated in the range 303–323 K. The data illustrate that the increase in temperature resulted in a decrease in the amount of Se(IV) adsorbed per unit mass of oxide adsorbents showing an exothermic nature of the adsorption process. The decrease in Se(IV) adsorption capacity with increasing temperature might be attributed to a change in surface properties of the adsorbent, solubility of the solute species and the exothermic nature of the adsorption process. Therefore, thermodynamic parameters were evaluated to assess the thermodynamic feasibility and to confirm the nature of the adsorption process. The thermodynamic parameters corresponding to Se(IV) adsorption on metal oxides were assessed using Van't Hoff equation [38]:

$$\log k_d = \frac{\Delta S^\circ}{2.303R} - \left(\frac{\Delta H^\circ}{2.303R}\right)\frac{1}{T} \tag{17}$$

Table 6
Thermodynamic parameters for adsorption of Se(IV) anions onto metal oxides.

Temperature (K)	Thermodynamic parameters					
	Iron oxide			Silicon oxide		
	ΔH° (kJ mol^{-1})	ΔG° (kJ mol^{-1})	ΔS° (J mol^{-1} K^{-1})	ΔH° (kJ mol^{-1})	ΔG° (kJ mol^{-1})	ΔS° (J mol^{-1} K^{-1})
303		17.61	202.25		16.76	170.77
313	43.67	16.89	193.50	34.98	16.07	163.10
323		15.88	184.38		15.56	156.47

where k_d is the distribution coefficient of the solute ions which equals to q_e/C_e, ΔS° is the entropy change (J mol^{-1} K^{-1}), R is the ideal gas constant (8.314 J mol^{-1} K^{-1}) and T is the absolute temperature in Kelvin. To evaluate the change in the standard enthalpy (ΔH°), a graph of log K_d versus $1/T$ was constructed. The figure shows straight lines with slopes equal to the value of ΔH° for the overall system. The magnitudes of other thermodynamic parameters were calculated at different temperatures, using the following equations, and listed in Table 6.

$$\Delta G^\circ = -2.303RT \log k_d \quad (18)$$

$$\Delta G^\circ = \Delta H^\circ - T\Delta S^\circ \quad (19)$$

The negative ΔG° values confirm the spontaneous nature and feasibility of the adsorption process. With the increase of temperature, the ΔG° value decreased from 17.61 to 15.88 kJ mol^{-1} for iron oxide and from 16.76 to 15.56 kJ mol^{-1} for silicon oxide. This indicates that favorable Se(IV) adsorption takes place with decreasing temperature. The negative ΔH° values indicate the exothermic nature of Se(IV) adsorption onto the applied oxides. The negative ΔS° values suggest the decrease in adsorbate concentration in solid-solution interface indicating thereby the increase in adsorbate concentration onto the solid phase. This is the normal consequence of the chemical sorption phenomenon, which takes place through ligand-exchange interactions as suggested earlier. Also, the negative values of ΔS° specify an increased randomness at the oxide/solution interface during the progress of adsorption process.

4. Conclusion

The present study shows that iron and silicon oxides could be used as an effective adsorbent for removal of selenite from aqueous solution and wastewaters. The quantitative removal of Se(IV) was highly attained from acidic solutions implying the efficiency of pH adjustment, as a pre-treatment, for potential removal of selenium from waste solutions using oxide adsorbents. The adsorption process follows pseudo-second-order kinetics. The removal of selenite anions by these metal oxides takes place via particle and film particle diffusion mechanisms, and the thermodynamic parameters reflect the feasibility of the process. The adsorption isotherms fitted well to the linear form of Freundlich, Langmuir and D–R isotherm models that best correlate the experimental data. The sorption of Se(IV) onto both metal oxides is an exothermic process and the results avouch that they can be fruitfully employed for the removal of Se anions in a wide range of concentrations. Generally, the analysis of experimental results by equilibrium sorption isotherms is important in developing accurate data that could be used for sorption design purposes. The adsorption parameters and the underlying thermodynamic assumptions of these equilibrium models often provide some insight into both the adsorption mechanism and the surface properties and affinity of the adsorbent.

Acknowledgment

The authors would like to express their thanks and gratitude to Prof. H. Someda, professor of radiochemistry, Head of Nuclear Chemistry Department, Hot Lab Center, AEA, for her keen interest.

Appendix A. Supplementary data

Supplementary data associated with this article can be found, in the online version, at doi:10.1016/j.cej.2010.03.004.

References

[1] N. Zhang, L.S. Lin, D. Gang, Adsorptive selenite removal from water using iron-coated GAC adsorbents, Water Res. 42 (14) (2008) 3809–3816.
[2] L. Zhao, G.H. Zhao, M. Du, Z.D. Zhao, L.X. Xiao, X.S. Hu, Effect of selenium on increasing free radical scavenging activities of polysaccharide extracts from a Se-enriched mushroom species of the genus, Eur. Food Res. Technol. 226 (2008) 499–505.
[3] W. Oliver, C. Fuller, D.L. Naftz, W.P. Johnson, X. Diaz, Estimating selenium removal by sedimentation from the Great Salt Lake, Utah, Appl. Geochem. 24 (5) (2009) 936–949.
[4] M. Lenz, E.C. Van Hullebusch, G. Hommes, F.X. Corvini, P.N.L. Lens, Selenate removal in methanogenic and sulfate-reducing upflow anaerobic sludge bed reactors, Water Res. 42 (2008) 2184–2194.
[5] Y.T. Chan, W.H. Kuan, T.Y. Chen, M.K. Wang, Adsorption mechanism of selenate and selenite on the binary oxide systems, Water Res. 43 (2009) 4412–4420.
[6] J. Das, B. Sairam-Patra, N. Baliarsingh, K.M. Parida, Calcined Mg–Fe–CO_3 LDH as an adsorbent for the removal of selenite, J. Colloid Interface Sci. 316 (2007) 216–223.
[7] M. Duc, G. Lefèvre, M. Fédoroff, Sorption of selenite ions on hematite, J. Colloid Interface Sci. 298 (2006) 556–563.
[8] Y. Jan, T. Wang, M. Li, S. Tsai, Y. Wei, S. Teng, Adsorption of Se species on crushed granite: a direct linkage with its internal iron-related minerals, Appl. Radiat. Isot. 66 (2008) 14–23.
[9] Y. Tamari, Methods of analysis for the determination of selenium in biological geological and water samples, in: W.T. Frankenberger Jr., R.A. Engberg (Eds.), Environmental Chemistry of Selenium, Marcel Dekker, Inc., 1998.
[10] L.W. Jacobs, Selenium in Agriculture and the Environment, American Society of Agronomy, Inc., Madison, WI, 1989.
[11] I. Pointeau, D. Hainos, N. Coreau, P. Reiller, Effect of organics on selenite uptake by cementitious materials, Waste Manage. 26 (2006) 733–740.
[12] K.H. Goh, T.T. Lim, Geochemistry of inorganic arsenic and selenium in a tropical soil: effect of reaction time, pH and competitive anions on arsenic and selenium adsorption, Chemosphere 55 (6) (2004) 849–859.
[13] D. Peak, Adsorption mechanisms of selenium oxyanions at the aluminum oxide/water interface, J. Colloid Interface Sci. 303 (2006) 337–345.
[14] D.F. Shriver, P. Atkins, C.H. Langford, Inorganic Chemistry, second Ed., Freeman, New York, 1994.
[15] W.T. Frankenberger, C. Amerhein, T.W. Fan, D. Flaschi, J. Glater, E. Kartinen, K. Kovac, E. Lee, H.M. Ohlendorf, L. Owens, N. Terry, A. Toto, Advanced treatment technologies in the remediation of seleniferous drainage waters and sediments, Irrigation Drainage Syst. 18 (1) (2004) 19–42.
[16] V. Mavrov, S. Stamenov, E. Todorova, H. Chmiel, T. Erwe, New hybrid electrocoagulation membrane process for removing selenium from industrial wastewater, Desalination 201 (2006) 290–296.
[17] H. Hayashi, K. Kanie, K. Shinoda, A. Muramatsu, S. Suzuki, H. Sasaki, pH-dependence of selenate removal from liquid phase by reductive Fe(II)–Fe(III) hydroxysulfate compound, green rust, Chemosphere 76 (5) (2009) 638–643.
[18] D. Peak, D.L. Sparks, Mechanisms of selenate adsorption on iron oxides and hydroxides, Environ. Sci. Technol. 36 (2002) 1460–1466.
[19] M. Duc, G. Lefevre, M. Fedoroff, J. Jeanjean, J.C. Rouchaud, F. Monteil-Rivera, J. Dumonceau, S. Miloniic, Sorption of selenium anionic species on apatites and iron oxides from aqueous solutions, J. Environ. Radioact. 70 (2003) 61–72.
[20] C.H. Wu, S.L. Lo, C.F. Lin, Competitive adsorption of molybdate, chromate, sulfate, selenate, and selenite on γ-Al_2O_3, Colloids Surf. A: Physicochem. Eng. Aspects 166 (2000) 251–259.
[21] T. Pullukat, R. Ho, Silica-based Ziegler–Natta catalysts: a patent review, Catal. Rev.: Sci. Eng. 41 (1999) 389–428.
[22] C. Su, D.L. Suarez, Selenate and selenite sorption on iron oxides: an infrared and electrophoretic study, Soil Sci. Soc. Am. J. 64 (2000) 101–111.

[23] F. Monteil-Rivera, M. Fedoroff, J. Jeanjean, L. Minel, M. Barthes, J. Dumonceau, Sorption of selenite (SeO_3^{2-}) on hydroxyapatite: an exchange process, J. Colloid Interface Sci. 221 (2000) 291–300.
[24] R.R. Sheha, E. Metwally, Equilibrium isotherm modeling of cesium adsorption onto magnetic materials, J. Hazard. Mater. 143 (2007) 354–361.
[25] M.A. Álvarez-Merino, V. López-Ramón, C. Moreno-Castilla, A study of the static and dynamic adsorption of Zn(II) ions on carbon materials from aqueous solutions, J. Colloid Interface Sci. 288 (2) (2005) 335–341.
[26] S.D. Faust, O.M. Aly, Chemistry of Natural Waters, Ann Arbor Science, Ann Arbor, MI, 1981.
[27] A. Manceau, L. Charlet, The Mechanism of selenate adsorption on goethite and hydrous ferric oxide, J. Colloid Interface Sci. 168 (1) (1994) 87–93.
[28] N. Jordan, C. Lomenech, N. Marmier, E. Giffaut, J.J. Ehrhardt, Sorption of selenium(IV) onto magnetite in the presence of silicic acid, J. Colloid Interface Sci. 329 (2009) 17–23.
[29] R.R. Sheha, A.A. El-Zahhar, Synthesis of some ferromagnetic composite resins and their metal removal characteristics in aqueous solutions, J. Hazard. Mater. 150 (2008) 795–805.
[30] L. Zhang, N. Liu, L. Yang, Q. Lin, Sorption behavior of nano-TiO_2 for the removal of selenium ions from aqueous solution, J. Hazard. Mater. 170 (2009) 1197–1203.
[31] E.I. El-Shafey, Sorption of Cd(II) and Se(IV) from aqueous solution using modified rice husk, J. Hazard. Mater. 147 (2007) 546–555.
[32] R.R. Sheha, H.H. Someda, Removal of some chelators from aqueous solutions using polymeric ingredients, Chem. Eng. J. 114 (2005) 105–113.
[33] A. El-Kamash, A. Zaki, M. Abdel Geleel, Modeling batch kinetics and thermodynamics of zinc and cadmium ions removal from waste solutions using synthetic zeolite A, J. Hazard. Mater. B127 (2005) 211–220.
[34] S.S. Gupta, K.G. Bhattacharyya, Adsorption of Ni(II) on clays, J. Colloid Interface Sci. 295 (1) (2006) 21–32.
[35] A. Benhammoua, A. Yaacoubi, L. Nibou, B. Tanouti, Adsorption of metal ions onto Moroccan stevensite: kinetic and isotherm studies, J. Colloid Interface Sci. 282 (2) (2005) 320–326.
[36] F. Helferich, Ion Exchange, McGraw Hill, New York, 1962.
[37] B.F. Noeline, D.M. Manohar, T.S. Anirudhan, Kinetic and equilibrium modelling of lead(II) sorption from water and wastewater by polymerized banana stem in a batch reactor, Sep. Purif. Technol. 45 (2005) 131–140.
[38] S.I. Lyubchik, A.I. Lyubchik, O.L. Galushko, L.P. Tikhonova, J. Vital, I.M. Fonseca, S.B. Lyubchik, Kinetics and thermodynamics of the Cr(III) adsorption on the activated carbon from co-mingled wastes, Colloids Surf. A: Physicochem. Eng. Aspects 242 (1–3) (2004) 151–158.